HHS Public Access

Author manuscript

Oncogene. Author manuscript; available in PMC 2021 March 28.

Published in final edited form as:

Oncogene. 2020 November ; 39(47): 7034–7050. doi:10.1038/s41388-020-01481-y.

Her2 promotes early dissemination of breast cancer by suppressing the p38 pathway through Skp2-mediated proteasomal degradation of Tpl2

Guanwen Wang[1,2,*], **Juan Wang**[1,2,*], **Antao Chang**[1,2], **Dongmei Cheng**[1], **Shan Huang**[1,2], **Dan Wu**[1], **Sherona Sirkisoon**[1], **Shuang Yang**[2], **Hui-Kuan Lin**[1], **Hui-Wen Lo**[1], **Rong Xiang**[2,#], **Peiqing Sun**[1,#]

[1]Department of Immunology, School of Medicine, Nankai University, Tianjin, China

[2]Department of Cancer Biology and Comprehensive Cancer Center, Wake Forest Baptist Medical Center, Winston-Salem, North Carolina, USA

Abstract

While mechanisms for metastasis were extensively studied in cancer cells from patients with detectable tumors, pathways underlying metastatic dissemination from early lesions before primary tumors appear are poorly understood. Her2 promotes breast cancer early dissemination by suppressing p38, but how Her2 downregulates p38 is unclear. Here, we demonstrate that in early lesion breast cancer models, Her2 inhibits p38 by inducing Skp2 through Akt-mediated phosphorylation, which promotes ubiquitination and proteasomal degradation of Tpl2, a p38 MAP3K. The early disseminating cells are $Her2^{+}Skp2^{high}Tpl2^{low}p\text{-}p38^{low}E\text{-}cadherin^{low}$ in the MMTV-Her2 breast cancer model. In human breast carcinoma, high Skp2 and low Tpl2 expression are associated with the $Her2^{+}$ status; Tpl2 expression positively correlates with that of activated p38; Skp2 expression negatively correlates with that of Tpl2 and activated p38. Moreover, the Her2-Akt-Skp2-Tpl2-p38 axis plays a key role in the disseminating phenotypes in early lesion breast cancer cells; inhibition of Tpl2 enhances early dissemination in vivo. These findings identify the Her2-Akt-Skp2-Tpl2-p38 cascade as a novel mechanism mediating breast cancer early dissemination and a potential target for novel therapies targeting early metastatic dissemination.

Keywords

Her2; Skp2; Tpl2; p38; early dissemination; breast cancer

[#]**Corresponding authors**: Peiqing Sun, psun@wakehealth.edu, Rong Xiang, rxiang@nankai.edu.cn.

[*]Equal contribution to the study

Author contributions

GW, JW, RX and PS conceived and designed the study. GW, JW, MD, SH, AC, and DW executed the experiments; GW, JW, AC, KL, SS, HL, HL and PS analyzed and interpreted the data. GW, JW, HL, HL, RX and PS wrote and/or reviewed the manuscript.

Conflict of interests

Authors declare no competing interests in relation to the work described.

Introduction

Metastasis is the leading cause of cancer-related deaths, which in the traditional views, occurs during late stages of tumor progression[1]. However, 2–3% of breast cancer patients who have been treated for ductal carcinoma in situ (DCIS), a noninvasive early lesion, die of metastasis without ever developing a primary tumor[2], suggesting that early metastasis occurs before or as DCIS develop. Increasing evidence suggests that tumor cells can disseminate from the earliest preneoplastic lesions, even in the absence of clinically detectable primary tumors, in multiple cancer types including melanoma, pancreatic cancer and breast cancer[3–8]. Thus, some non-invasive lesions by historical definition such as DCIS, can be invasive and metastatic in nature. While pathways underlying metastasis have been extensively studied in cancer cells isolated from patients with detectable primary tumors, mechanisms mediating dissemination and metastasis of early cancer lesions are poorly understood.

Epithelial-mesenchymal transition (EMT) is important for epithelial tumor cells to lose polarity and cell-cell adhesions, leading to disruption of normal tissue architecture and initiation of metastatic dissemination[9, 10]. A key mechanism for EMT is activation of β-catenin, a transcription factor in the Wnt signaling pathway, which interacts with E-cadherin at adherent junctions to maintain cell-cell contact and epithelial properties[11]. Phosphorylation of β-catenin by Src results in its dissociation from E-cadherin and translocation into the nucleus [12], where it induces transcription of pro-EMT genes that suppress E-cadherin expression, leading to disruption of cell-cell contact and EMT[13]. Activated Wnt signaling suppresses GSK3β-mediated phosphorylation and degradation of β-catenin protein leading to its stabilization and accumulation in the nucleus[13].

Mitogen-activated protein kinases (MAPKs) are sequentially activated through phosphorylation by a cascade of protein kinases, including MAPK kinase kinases (MAP3Ks) and MAPK kinases (MAP2Ks). Several MAP3Ks have been shown to induce p38 MAPK activation through MAP2Ks MKK3 and MKK6 [14], including ASK1, DLK1, TAO1 and 2, Tpl2, MLK2, MLK3, MEKK3, MEKK4, and ZAK1[15]. p38 regulates cellular functions through phosphorylation of downstream substrates, including transcription factors including ATF2, and serine/threonine protein kinases including PRAK and MK2 that phosphorylates a small heat shock proteins Hsp27[16]. Tpl2 (tumor progression loci 2) was identified as MAPK3K initially for ERK [17–19], and later for p38[20, 21]and JNK [18, 22]. Tpl2 also phosphorylates NF-kB1(p105)-Ser933, and prompts its proteolysis to p50[23, 24]. Tpl2 activity is induced by IKKβ-mediated phosphorylation of Ser290[25]. Also, Tpl2 is sequestered in a complex with NF-κB1-p105 and ABIN2; upon NF-κB1-p105 phosphorylation by IKKβ, Tpl2 is released from the complex resulting in activation of MKK3/6[20].

The role of the p38 pathway in cancer and metastasis is highly context-dependent. While it was initially considered cancer-promoting, especially in late-stage cancer development, later studies reported that it suppresses cancer[26–30]. In established cancer cell lines, p38 promotes cancer cell migration/metastasis[31–33], but in cell and mouse models for early

lesion breast cancer, p38 suppresses Her2-mediated early dissemination[34]. Thus, p38 plays differential roles in the metastasis of early lesions and late-stage breast cancer.

The role of Tpl2 in cancer is also context-dependent. Tpl2 promotes cancer progression by phosphorylating Pin1 resulting cyclin D1 upregulation [35] and induces EMT through ERK and JNK in breast cancer cells[35, 36], but $Tpl2^{-/-}$ mice display increased two-stage skin carcinogenesis[37]. Tpl2 also suppresses lung carcinogenesis, with downregulated expression in human lung cancer[38].

In this study, we investigated the mechanism underlying breast cancer early dissemination using cell and mouse models of early lesion breast cancer. MCF-10A cells, a non-transformed human breast epithelial cell line can form acini-like structures containing a single layer of polarized, growth-arrested cells when grown in Matrigel which mimic the acini in adult breasts; Her2 overexpression leads to disrupted acinar structures that share properties with DCIS in vivo including uncontrolled cell proliferation and luminal filling, without invasion. MCF-10A-Her2 is thus a useful model for early-stage carcinogenesis in vitro[39]. The MMTV-Her2 transgenic mouse model, expressing rat *Her2/neu* gene driven by MMTV promoter, develops mammary lesions that progress through three stages, atypical hyperplasia, mammary intraepithelial neoplasia (similar to human DCIS) and invasive carcinoma. Epithelial hyperplasia is detected microscopically in mammary glands around week-7–9; in situ carcinomas occur at week-18. Tumors in mammary glands start to become palpable around week-20, invasive cancers become apparent at week-23–30, and 72% of tumor-bearing mice that live beyond 8 months develop lung metastasis[40]. While a recent study showed that Her2 promotes early dissemination by suppressing p38[34], it is unclear how Her2 suppresses p38 during early dissemination. We demonstrate that Her2 downregulates p38 activity by targeting the Tpl2 protein for Skp2-mediated degradation upon activation of Skp2 by Her2 and Akt, and that decreased Tpl2 expression induced by the Her2-Akt-Skp2 pathway plays a key role in inhibiting p38 and promoting migration, invasive and EMT in cells and early dissemination in vivo. These findings provided novel insights into the mechanism underlying breast cancer early dissemination, identified a novel substrate and biological function of Skp2, and revealed a targetable pathway for treating breast cancer early dissemination and metastasis.

Results

Reduced levels of a p38 MAP3K Tpl2 correlates with $Her2^+$ status and reduced p38 activation in cell and mouse models of breast cancer early lesions and human breast cancer tissues

We investigated the mechanism underlying Her2-mediated p38 downregulation in early lesion breast cancer cells. Since all existing $Her2^+$ breast cancer cell lines were derived from established, detectable tumors and do not represent early lesion cancer cells, we used MCF-10A mammary epithelial cells transduced with Her2 and mammary epithelial cells isolated from MMTV-Her2 mice with early lesions to model early lesion breast cancer cells. The levels of ectopic Her2 expression was comparable to or less than that in a naturally occurring $Her2^+$ breast cancer cell line SK-BR-3 (Fig. S1A). Thus, Her2 effects observed in these early lesion cells cannot be artifacts due to gross Her2 overexpression. Her2 was

barely detectable in mammary epithelial cells from FVB mice, a $Her2^{-}$ human breast cancer cell line MDA-MB-231, control MCF-10A cells, and normal human mammary epithelial cells (HMECs).

To identify the starting point of Her2 regulation in the p38 pathway, we searched for p38 upstream regulators whose expression, rather than phosphorylation, is altered by Her2, because changes in phosphorylation of a protein is likely due to Her2-induced changes in an upstream protein, and thus this protein may not be the starting point of Her2 action in the p38 pathway. In a survey of p38 upstream regulators, ectopically expressed Her2 decreased phosphorylation but not expression of MKK3/6, reduced the protein but not mRNA levels of Tpl2, both protein and mRNA levels of MLK2, MLK3 and MEKK4, and the mRNA but not the protein levels of MEKK3, TAK1, TAO2 and TAB1β in MCF-10A cells (Fig. 1A, S1B–C). Genes upregulated by Her2 or without changes in protein were not pursued. Decreased mRNA levels for MLK2, MLK3 and MEKK4 did not correlate with the $Her2^{+}$ status in breast cancer in GEO database (Fig. S1D), and thus they were not further analyzed.

We analyzed Tpl2 and confirmed the Her2-mediated reduction in Tpl2 protein in mammary epithelial cells isolated from wild type and MMTV-Her2 mice (Fig. 1B). Her2 inhibition by Lapatinib increased levels of Tpl2, phospho-p38 and -Hsp27 and E-cadherin, and decreased Vimentin in MCF-10A-Her2 cells (Fig. S1E), conforming that Her2 inhibits the Tpl2-p38 pathway and promotes EMT. As reported[34], mammary glands of 14–18-week-old MMTV-Her2 mice had no palpable tumors, but displayed early lesions (hyperplasia and mammary intraepithelial neoplasia) (Fig. S1F) and early dissemination of $Her2^{+}$ tumor cells to the lung (Fig. S1G–H). About 78% of the $Her2^{high}$ cells in the MMTV-Her2 mammary ducts, 83% of the $Her2^{high}$ cells in invading buds in MMTV-Her2 early lesions, and all the $Her2^{+}$ cells disseminated to the lung contained very low or undetectable Tpl2 levels (Fig. 1C–E). Most $Tpl2^{low}$ cells were also E-$cadherin^{low}$ in MMTV-Her2 mammary ducts (Fig. 1F), suggestive of their EMT and disseminating phenotype. Thus, these $Her2^{high}$ early disseminating cells are $Tpl2^{low}$ in MMTV-Her2 mice.

We investigate the relationship among Her2, Tpl2 and phospho-p38 in human breast cancer, using human breast cancer tissue arrays containing early lesions (atypical ductal hyperplasia, or ADH, and DCIS) or late-stage carcinoma tissues. Low Tpl2 expression correlated with the $Her2^{+}$ status (Fig. 1G–H, S1I–J) and with low levels of activated p38 (p-p38) (Fig. 1I, S1K) in both early and advanced lesions. Therefore, suppression of Tpl2 by Her2 likely contributes to p38 inactivation and early dissemination in human breast cancer.

Tpl2 suppresses Her2-mediated migration, invasion and EMT in early lesion cells

We examined the effect of Tpl2 overexpression and knockdown in early lesion breast cancer cells. Ectopic expression of Tpl2 increased phosphorylation of MKK3/6, p38 and Hsp27 and E-cadherin expression and junctions, and reduced migration and percentage of organoids with outward invading cells (Fig. 2A–D), while Tpl2 knockdown had opposite effects (Fig. 2E–H), in MMTV-Her2 cells. Similar observations were made in MCF-10A and MCF-10A-Her2 cells. Ectopic expression of Tpl2 upregulated MKK3/6, p38 and Hsp27 phosphorylation and suppressed migration, invasion and EMT (Fig. S2A–F), while Tpl2 knockdown had opposite effects (Fig. S3A–E). Also, Tpl2 reduced and Tpl2 shRNAs

increased the level of Vimentin, a mesenchymal cell marker (Fig. S2A, S3A). Consistent with reports that p38 suppresses breast cancer cell early dissemination by inhibiting β-catenin activation[34], Tpl2 overexpression reduced the levels of activated β-catenin (Fig. S2G) and promoted translocation of β-catenin from nuclei to cell surface (Fig. S2H), while the Tpl2 shRNAs had opposite effects (Fig. S3F–G), in MCF-10A and MCF-10A-Her2 cells. Tpl2 reduced expression of stemness-related transcription factors SOX2 and OCT4 and a cancer stemness marker ALDHA1 in MCF-10A-Her2 cells (Fig. S2I), while Tpl2 shRNAs increased their expression in MCF-10A cells (Fig. S3H), supporting the impact of EMT on cancer cell stemness[41].

In SK-BR-3, a $Her2^+$ metastatic breast adenocarcinoma cell line, Tpl2 overexpression activated MKK3/6 and p38, but downregulated E-cadherin and upregulated Vimentin and cell migration (Fig S2J–K), consistent with the reported metastasis-promoting function of p38 in late stage breast cancer cells[42, 43], suggesting that Tpl2 and p38 have opposite roles in metastatic dissemination in early and late lesions of breast cancer.

As reported[34], Her2 enhanced migration, invasion, EMT and β-catenin activation, as compared to vector control, in MCF-10A cells (Fig. S2–3). Her2-induced changes in the levels of phospho-MKK3/6/p38/Hsp27, E-cadherin and Vimentin, migration, invasive organoids, E-cadherin junctions and β-catenin activation and nuclear localization were abrogated by Tpl2 overexpression (see quantifications of Fold Changes by Her2, Fig. S2A–H) in MCF-10A cells, indicating that Tpl2 downregulation is essential for Her2 to suppress the p38 pathway and promote invasion/EMT. Tpl2 shRNAs alone were sufficient to suppress the p38 pathway and promote migration/invasion, EMT, β-catenin activation and stemness in MCF-10A cells without Her2, and further enhanced the Her2 effects on p38 and these phenotypes in MMTV-Her2 and MCF-10A-Her2 cells (Fig. 2E–H, S3A–H). These findings, along with the reduction of Tpl2 expression by Her2 (Fig. 1A–B), demonstrate that despite that Her2 activates multiple signaling networks, it suppresses p38 and induces the disseminating phenotypes at least partly by downregulating Tpl2 expression in early lesion cells of breast cancer. Supporting the notion that Her2-mediated Tpl2 downregulation contributes to breast cancer early dissemination in vivo, most $Her2^+Tpl2^{low}$ cells in the mammary ducts of MMTV-Her2 mice were also low or negative for E-cadherin, indicative of their disseminating nature (Fig. 1F).

Despite reports that Tpl2 phosphorylates other MAPKs and NF-κB1(p105)-Ser933 besides p38, and that NF-κB1(p105)-Ser933 phosphorylation leads to proteolysis of NF-κB1(p105) to NF-κB1(p50)[18, 19, 24, 44], Tpl2 overexpression/knockdown did not significantly upregulate MEK, NF-κB1, ERK or JNK phosphorylation or the total levels of NF-κB1(p105) or NF-κB1(p50) in MCF-10A/MCF-10A-Her2 cells (Fig. S2A, S3A), suggesting that Tpl2 does not activate these pathways in these conditions. We further determined the epistatic relationship among Her2, Tpl2, MKK3/6 and p38. While dominant-negative MKK6A alone without Her2 reduced p-p38, p-Hsp27 and E-cadherin expression and junctions and increased invasive organoids and further enhanced the effects on Her2 on these phenotypes (Fig. 2I–K), constitutively active MKK6E abrogated Her2-induced decreases in p-p38 and E-cadherin junctions and increases in invasive organoids (Fold Changes by Her2, Fig. 2L–N). Thus, MKK6 downregulation is both sufficient, and necessary for Her2, to

suppress p38 and promote invasion/EMT. Moreover, MKK6A abrogated Tpl2-induced increase in p-p38, p-Hsp27 and E-cadherin expression and junctions and decrease in invasive organoids (Fold Changes by Tpl2, Fig. 2I–K; in Fig. 2K, Tpl2-induced changes in E-cadherin junctions was significant in control cells but insignificant in MKK6A cells); and MKK6E abrogated Tpl2 shRNA-induced decreases in p-p38, p-Hsp27 and E-cadherin junctions and increase in invasive organoids (Fold Changes by shTpl2, Fig. 2L–N; in Fig. 2M, shTpl2-induced changes in invasion was significant in control Her2-cells but insignificant in MKK6E-Her2 cells), in MCF-10A and MCF-10A-Her2 cells. MKK6A/E had no effect on Tpl2 expression (Fig. 2I, 2L). Therefore, Tpl2 suppresses invasion and EMT at least partly by activating MKK3/6-p38 pathway.

MAPK phosphatase1 (MKP1) is the prototype of the dual specificity phosphatase (DUSP) family, which dephosphorylates MAPKs[45] and is induced by Her2 in breast cancer through protein stabilization via ERK-mediated MKP1-Ser359 phosphorylation[46]. Although Her2 increased p-MKP1(S359) and MKP1 levels in MCF10A cells (Fig. S1B), MKP1 shRNAs slightly increased JNK phosphorylation without affecting p38 or ERK phosphorylation, migration, invasion, E-cadherin junctions or β-catenin activation in MCF-10A-Her2 cells (Fig. S3I–M). Thus, MKP1 is not a major regulator of Her2-mediated p38 suppression and metastasis in early lesion breast cancer cells.

Her2 reduces Tpl2 protein stability through Skp2-mediated protein ubiquitination and proteasomal degradation in early lesion cells.

We investigated the mechanism by which Her2 downregulates Tpl2. Ectopic expression of Her2 did not alter the level (Fig. S1B) or stability (Fig. S4A) of Tpl2 mRNA, but reduced Tpl2 protein stability (Fig. S4B–C). A proteasome inhibitor MG132 increased Tpl2 protein in MCF-10A cells and decreased Her2-induced fold reduction in Tpl2 protein (Fig. S4D), suggesting that both basal and Her2-induced Tpl2 protein degradation is proteasome-mediated.

Skp2 is an oncogenic E3 ubiquitin ligase targeting proteins including p27 for proteasomal degradation[47]. Skp2 activity is upregulated by Akt [48, 49], which is activated by Her2 and was implicated in Her2-mediated p38 suppression and breast cancer early dissemination[34]. Her2 upregulated Skp2 protein in MMTV-Her2 and MCF-10A-Her2 cells representing early lesions, compared to respective controls (Fig. S4E–F). shRNA-mediated Skp2 knockdown increased Tpl2, p-p38 and p-Hsp27 levels in MMTV-Her2 cells (Fig. 3A) and abrogated Her2-induced decreases in Tpl2, p-p38 and p-Hsp27 in MCF-10A cells (Fig. 3B, Fold reduction by Her2), compared to control shRNAs. Overexpression of wild type, but not the catalytically inactive mutants (Skp2-NES and -LRR)[50] of, Skp2 alone was sufficient to reduce Tpl2, p-p38 and p-Hsp27 in MCF-10A cells and further enhanced the Her2 effects on these proteins in MMTV-Her2 and MCF-10A-Her2 cells (Fig. 3C–E). Thus, Skp2 induction is both sufficient, and necessary for Her2, to downregulate the Tpl2-p38 pathway. Skp2 shRNAs also increased Tpl2, p-p38 and p-Hsp27 in MCF-10A cells (Fig. 3B), suggesting that the basal Skp2 level, whether regulated by endogenous Her2 or not, is sufficient to inhibit Tpl2-p38 activity.

Tpl2 or Skp2 was detected in the protein complex immunoprecipitated by an antibody against Skp2 or Tpl2 (Fig. 3F–G), respectively, indicating interaction between endogenous Skp2 and Tpl2. In MCF-10A cells, Skp2 shRNAs abrogated Her2-induced Tpl2 protein ubiquitination, while the wild type, but not the catalytically inactive mutants of, Skp2 increased Tpl2 ubiquitination (Fig. 3H–I). These data thus identify Skp2 as an E3 ubiquitin ligase for Tpl2.

In MMTV-Her2 mice with early lesions, most $Her2^{high}$ cells in mammary ducts, most $Her2^{high}$ cells in invading buds in the early lesions, and all the $Her2^{+}$ cells disseminated to the lung contained high Skp2 levels (Fig. 3J–L); and most of the $Skp2^{high}$ cells had low Tpl2 levels in mammary ducts (Fig. 3M). In both early-lesion and late-stage human breast cancer tissues, high Skp2 expression correlated with the $Her2^{+}$ status (Fig. 1J, S1L) and low Tpl2 (Fig. 1K, S1M) and p-p38 (Fig. 1L, S1N) levels, suggesting that the Her2-Skp2-Tpl2-p38 axis likely contributes to early dissemination of human breast cancer.

Together, our results demonstrate that Tpl2 is a novel substrate of Skp2, and that Her2 upregulates Skp2, and reduces Tpl2 protein expression through Skp2-mediated ubiquitination and proteasomal degradation in early disseminating breast cancer cells.

Skp2 promotes Her2-mediated migration, invasion and EMT by suppressing Tpl2 in early lesion cells

We investigated the role of Skp2-mediated Tpl2 suppression in Her2-induced disseminating phenotypes. Skp2 knockdown increased E-cadherin expression and junctions and reduced Vimentin expression, migration and percentage of invasive organoids in MMTV-Her2 cells (Fig. 4A–D), and abrogated Her2-induced decreases in E-cadherin expression and junctions and increases in migration, invasive organoids and nuclear translocation and activation of β-catenin in MCF-10A cells (Fold Changes by Her2, Fig. 4E–H, S5A–C). Ectopic expression of wild type, but not the catalytically inactive mutants of, Skp2 alone increased Vimentin expression, migration, invasive organoids and β-catenin nuclear translocation and activation, and reduced E-cadherin expression and junctions in MCF-10A cells and enhanced the Her2 effects on some of these phenotypes in MCF-10A-Her2 cells (Fig. 4I–O, S5D–G). Wild type Skp2 also reduced E-cadherin expression and junctions in MMTV-Her2 cells (Fig. 4P–Q). Skp2 knockdown reversed Her2-mediated increase in SOX2, OCT4 and ALDHA1 expression in MCF-10A-Her2 cells (Fig. S5H–I), while wild type, but not catalytically-inactive mutants of, Skp2 alone induced these proteins in MCF-10A cells (Fig. S5J). Thus, Skp2 induction is both sufficient, and necessary for Her2, to promote migration, invasion and EMT in early lesion breast cancer cells. Skp2 shRNAs also moderately altered some, but not all, of these disseminating phenotypes (e.g., E-cadherin junctions and migration, Fig. 4E–F, H) in MCF-10A cells, suggesting that the basal Skp2 levels also regulate these phenotypes.

We determined the epistasis between Skp2 and Tpl2 in migration/invasion. Tpl2 knockdown abrogated Skp2 shRNA-induced increases in Tpl2, p-MKK3/6, p-p38, p-Hsp27 and E-cadherin levels and E-cadherin junctions and decreases in invasive organoids in MMTV-Her2 and MCF-10A-Her2 cells (Fig. 5A–F, Fold Changes by shSkp2), while Tpl2 overexpression abrogated Skp2-induced decreases in Tpl2, p-MKK3/6, p-p38, p-Hsp27 and

E-cadherin levels and E-cadherin junctions and increases in invasive organoids in MCF-10A cells (Fig. 5G–I, Fold Changes by Skp2). These rescue studies established an epistatic order of Her2-Skp2-Tpl2 in Her2-mediated migration/invasion in early lesion breast cancer cells. Tpl2 knockdown and overexpression alone downregulated and upregulated the p38 pathway and promoted and suppressed invasion/EMT, respectively, in cells without Skp2 manipulations, suggesting that the basal Tpl2 level is sufficient to activate p38 and promote invasion/EMT, and is not saturated for its function, respectively.

Further supporting the role of Skp2 in early dissemination in vivo, over 85% of the $Skp2^{high}$ cells were E-$cadherin^{low}$ in early lesions of the MMTV-Her2 mammary tissues (Fig. 5J), suggesting an EMT and disseminating phenotype of this group of $Her2^{+}Skp2^{high}Tpl2^{low}$ cells in this model.

Her2 promotes Skp2 expression and function through Akt-mediated phosphorylation.

We investigate the mechanism by which Her2 regulates Skp2. Her2 inhibits p38 through its well-known downstream effectors PI3K/Akt during breast cancer early dissemination[34, 51]. Increased Skp2 expression correlates with elevated PI3K/Akt activity in cancer [47]; and Akt phosphorylates Skp2-Ser72, which promotes Skp2 cytoplasmic localization and protein stabilization by protecting it from Cdh1-mediated degradation[48, 49]. Indeed, Her2 increased Skp2 protein and Akt activation in early lesion breast cancer cells (Fig. S4E–F). Her2-induced Skp2 phosphorylation was reduced by Akt inhibitor MK2206 [52] in MCF-10A cells (Fig. 6A), indicating that Her2-mediated Skp2 phosphorylation requires Akt. PI3K inhibitor GDC-0941 [34] and MK2206 abrogated Her2-induced increase in Skp2 proteins and decreases in Tpl2 and p-p38 levels (Fold Change by Her2, Fig. 6B) without inducing apoptosis (Fig. S6), while constitutively active Akt upregulated Skp2 and downregulated Tpl2, p-p38 and p-Hsp27 in both MCF-10A and MCF-10A-Her2 cells (Fig. 6C). Thus, PI3/Akt activation is alone sufficient, and is required for Her2, to induce Skp2 and suppress Tpl2-p38. Overexpression of wild type Skp2, but not that carrying a non-phosphorylatable mutation at Ser72 (S72A) [49], reduced Tpl2, p-p38 and p-Hsp27 levels and E-cadherin expression and junctions, and increased Vimentin, cell migration, invasive organoids and β-catenin activation in MCF-10A-Her2 cells (Fig. 6D–I). Skp2 carrying phosphomimetic mutation at Ser72 (S72D)[49] behaved similarly to wild type Skp2 (Fig. 6D–I), likely because Ser72-phosphorylation is necessary, but not sufficient, to fully activate Skp2 in this pathway. Moreover, high Akt expression correlated with the $Her2^{+}$ status, high Skp2 expression and low Tpl2 expression in human breast cancer tissues (Fig. S1O–R). Thus, Akt-mediated Skp2 phosphorylation is required for its Her2-induced expression and function in Tpl2 degradation and suppression of the p38 pathway, and for its ability to promote the disseminating phenotypes in $Her2^{+}$ early lesion cells.

Pharmacological inhibition of Tpl2 promotes early dissemination in vivo.

As Tpl2 inhibition alone will not lead to cancer in mice and inhibition of Tpl2 by Her2 is unlikely to be complete in MMTV-Her2 mice, we tested whether further inhibition of Tpl2 by a Tpl2 inhibitor[21] would enhance early dissemination in vivo. In vitro, the Tpl2 inhibitor reduced p38 and Hsp27 phosphorylation but not MEK1/2, NF-κB1, ERK and JNK phosphorylation or the total levels of NF-κB1(p105) and NF-κB1(p50), increased migration,

invasive organoids and β-catenin activation, and decreased E-cadherin junctions in MMTV-Her2, MCF-10A and MCF-10A-Her2 cells (Fig. 7A–D, S7A–E), validating the efficacy of the inhibitor in vitro.

Compared to vehicle, the Tpl2 inhibitor reduced p38 and Hsp27 phosphorylation without affecting ERK and JNK (Fig. 7E) in mammary epithelial cells isolated from 14–18-week-old MMTV-Her2 mice with early lesions and reduced E-cadherin expression and increased nuclear β-catenin levels in mammary glands (Fig. 7F–G). The inhibitor did not alter proliferation of MCF-10A and MCF-10A-Her2 cells (Fig. S7F) and percentage of ducts with early lesions in the mammary glands (Fig. S7G), but increased the numbers of the $Her2^+$ early disseminating cancer cells (eDCCs) in blood, bone marrow and lungs (Fig. 7H–J). No micro or macro metastasis appeared in the lung at these early time points used to detect early dissemination (Fig. S7H). Thus, Tpl2 inhibits early dissemination of breast cancer cells in vivo.

Discussion

Early dissemination was reported in breast cancer, pancreatic cancer [8] and melanoma [7], but its underlying mechanism is poor understood. A recent study reported that Her2 promotes early dissemination by suppressing p38 that inhibits disseminating phenotypes[34]. Here, we show that Her2 suppresses p38 activity by promoting proteasomal degradation of Tpl2, a p38 MAP3K, through an E3 ubiquitin-protein ligase Skp2 that is induced by Akt-mediated phosphorylation upon Her2 activation (Fig. S7I). We demonstrated the role of the Her2-PI3K/Akt-Skp2-Tpl2-MKK3/6-p38 axis in migration, invasion and EMT in vitro and in early dissemination in vivo. We observed correlations among the $Her2^+$ status, high Skp2 levels, and low Tpl2 and p-p38 levels in early lesion tissues of human breast cancer, suggesting that Tpl2 suppression by Her2-induced Skp2 likely contributes to p38 inactivation and early dissemination in the human disease. These correlations were also observed in late-stage human breast cancer tissues suggesting that this pathway is preserved in advanced stages, although its metastasis-suppressing function may not be, as Tpl2 promoted migration in SK-BR-3 cells representing late-stage cancer. Decreased Tpl2 expression also associated with the $Her2^+$ status in breast cancer in a previous study using a small sample size[53]. Together, these studies have identified novel mediators of the p38 pathway that limits breast cancer early dissemination, providing new mechanistic insights into cancer metastasis and revealing potential targets for new cancer therapies that block early-stage metastasis.

The roles of Tpl2 and p38 in cancer are highly context dependent. The migration-promoting function of Tpl2 in SK-BR-3 cells is consistent with its reported ability to enhance cancer progression and EMT in breast cancer cells from late-stage patients[35, 36]. Our observation that Tpl2 reduces early dissemination and associated phenotypes in early lesions of breast cancer mirror the reported tumor-suppressing function of Tpl2[37, 38]. Similarly. p38 promotes metastatic phenotypes in established cell lines from multiple cancers[54], but suppresses breast cancer early dissemination in the MMTV-Her2 model and EMT, migration and invasion in early lesion breast cancer cell[30, 34, 55]. The parallel functions of Tpl2 and

p38 in metastasis in early and late lesions of cancer suggest that they likely act in the same pathway to regulate cancer metastasis.

In addition to p38, Tpl2 also phosphorylates ERK, JNK and NF-κB1(p105)-Ser933[24]. However, ERK, JNK and NF-κB1(p105) phosphorylation was not altered by Tpl2 overexpression or knockdown or Tpl2 inhibitor in early lesion breast cancer cells and in MMTV-Her2 animals. Thus, Tpl2 is likely a specific MAP3K for p38 in early lesion breast cancer cells and tissues. Lack of changes in ERK phosphorylation upon Tpl2 manipulations contradicted a report that p38 inhibition induced ERK1/2 phosphorylation as a negative feedback in MCF-10A and MEF cells [30]. Possibly, manipulations of Tpl2 and MKK6/p38 may not have same effects on the p38 signaling strength or the negative feedback involving p38 and ERK. Alternatively, the discrepancy may be caused by cell line specificity and/or stable vs transient p38 inhibition.

Our finding that MKP1 is dispensable for Her2-mediated p38 suppression and metastasis in early lesion cells does not rule out the involvement of other DUSP members or other proteins that regulate p38. However, our rescue experiments clearly show that p38 inhibition reversed the ability of Tpl2 to suppress the disseminating phenotypes, while activation of p38 reversed the ability of Tpl2 shRNAs to induce these phenotypes, demonstrating that Tpl2 suppresses the disseminating phenotypes at least in part via p38.

Tpl2 activation requires Ser290-phosphorylation by Ikkβ[17]. While reduction in Tpl2 protein levels by Her2 or Tpl2 shRNAs will certainly abrogate Tpl2 activity and its function in suppressing early dissemination, ectopic Tpl2 expression also stimulated the p38 pathway and suppressed disseminating phenotypes in our studies. It is thus highly likely that the cellular machinery mediating the activating phosphorylation of Tpl2 is not rate-limiting and is not suppressed by Her2 in mammary epithelial cells, suggesting that Her2 suppresses Tpl2 mainly by downregulating its protein expression, but not phosphorylation.

Our data indicate that Her2 reduces Tpl2 expression by inducing Skp2 through Akt-mediated phosphorylation, to promote early dissemination. Besides other known protein substrates[56], we have identified Tpl2 as a novel substrate of Skp2, and demonstrated that the ability of Skp2 to promote disseminating phenotypes upon activation by Her2 relies on suppression of Tpl2 in early lesion breast cancer cells, as silencing or overexpression of Tpl2 reversed the effect of Skp2 knockdown or overexpression, respectively, on dissemination in rescue studies.

Her2 can activate PI3K/Akt pathway through second messenger pathways including Ras or Grb2 or by direct binding to PI3K[51]. Activated Akt in turn phosphorylates Skp2-Ser72, protecting Skp2 from Cdh1-mediated degradation and promotes cytoplasmic localization of Skp2 [48]. We found that activating phosphorylation of Akt (Fig. S4E–F) and Akt-dependent phosphorylation of Skp2 (Fig. 6A) were both induced by Her2 in early lesion breast cancer cells. Importantly, PI3K/Akt-mediated phosphorylation of Skp2-Ser72 was essential for the ability of Skp2 to suppress Tpl2-p38 and to promote the disseminating phenotypes (Fig. 6), thus establishing the role of the Her2-PI3K/Akt-Skp2-Tpl2 pathway in early dissemination. However, PI3K/Akt inhibitors abrogated Her2-induced increase in Skp2 and reduction in

Tpl2 and p-p38, but did not alter the Her2-effect on p-Hsp27 in MCF-10A cells. It is possible that Hsp27 phosphorylation is regulated by Her2/PI3K/Akt in a more complicated fashion, or is affected by compensatory feedback mechanisms or by the non-specific activity of the inhibitors. Moreover, while we cannot rule out that Akt-mediated phosphorylation also promotes Skp2 cytoplasmic localization, PI3K and Akt were clearly required for induction of Skp2 expression (Fig. 6B–C), which at least partly contributes to Skp2 function in p38 suppression and early dissemination. Given the complicated nature of the PI3K-Akt network, further analyses, including rescue studies, are needed to determine whether PI3K-Akt is the only or major pathway mediating Her2-induced Skp2 activation, p38 suppression and early dissemination.

Materials and Methods

Reagent

MCF-10A-LXSN and MCF-10A-Her2 cells were treated with 5 μM actinomycin D (Sigma) [57], 10 μg/ml cycloheximide (Sigma)[48], 10 μM MG132 (Sigma)[58], 1 μM or 5 μM Tpl2 inhibitor (Calbiochem)[21], 2 μM Lapatinib (Selleckchem)[59] for mRNA stability assays, protein stability assays, and inhibition of Tpl2 and Her2 respectively. For treatment in mice, Tpl2 inhibitor was dissolved in 5% Cremophor/50 mM citric acid[21]. Sequences for primers used in this study are provided in Supplementary Table S1 and S2.

Additional materials and methods are provided in Supplementary Information.

Supplementary Material

Refer to Web version on PubMed Central for supplementary material.

Acknowledgements

We thank Cell Engineering and Tumor Tissue and Pathology Shared Resources of WFBCCC for support. This study was supported by NIH/NCI grants CA131231, CA172115, and P30CA012197 (PS) and Bilateral Inter-Governmental S&T Cooperation Project grants from Ministry of Science and Technology of China (81972882 and 2018YFE0114300) (RX). PS is an Anderson Oncology Research Professor.

References

1. Fidler IJ. The pathogenesis of cancer metastasis: the ‘seed and soil’ hypothesis revisited. Nat Rev Cancer 2003; 3: 453–458. [PubMed: 12778135]
2. Narod SA, Iqbal J, Giannakeas V, Sopik V, Sun P. Breast Cancer Mortality After a Diagnosis of Ductal Carcinoma In Situ. JAMA Oncol 2015; 1: 888–896. [PubMed: 26291673]
3. Pantel K, Brakenhoff RH. Dissecting the metastatic cascade. Nat Rev Cancer 2004; 4: 448–456. [PubMed: 15170447]
4. Abbruzzese JL, Abbruzzese MC, Hess KR, Raber MN, Lenzi R, Frost P. Unknown primary carcinoma: natural history and prognostic factors in 657 consecutive patients. J Clin Oncol 1994; 12: 1272–1280. [PubMed: 8201389]
5. Riethmuller G, Klein CA. Early cancer cell dissemination and late metastatic relapse: clinical reflections and biological approaches to the dormancy problem in patients. Semin Cancer Biol 2001; 11: 307–311. [PubMed: 11513566]
6. Lopez-Lazaro M The migration ability of stem cells can explain the existence of cancer of unknown primary site. Rethinking metastasis. Oncoscience 2015; 2: 467–475. [PubMed: 26097879]

7. Eyles J, Puaux AL, Wang X, Toh B, Prakash C, Hong M et al. Tumor cells disseminate early, but immunosurveillance limits metastatic outgrowth, in a mouse model of melanoma. J Clin Invest 2010; 120: 2030–2039. [PubMed: 20501944]
8. Kang Y, Pantel K. Tumor cell dissemination: emerging biological insights from animal models and cancer patients. Cancer Cell 2013; 23: 573–581. [PubMed: 23680145]
9. Thiery JP, Acloque H, Huang RY, Nieto MA. Epithelial-mesenchymal transitions in development and disease. Cell 2009; 139: 871–890. [PubMed: 19945376]
10. Vleminckx K, Vakaet L Jr., Mareel M, Fiers W, van Roy F. Genetic manipulation of E-cadherin expression by epithelial tumor cells reveals an invasion suppressor role. Cell 1991; 66: 107–119. [PubMed: 2070412]
11. Aberle H, Schwartz H, Kemler R. Cadherin-catenin complex: protein interactions and their implications for cadherin function. J Cell Biochem 1996; 61: 514–523. [PubMed: 8806074]
12. Behrens J, Vakaet L, Friis R, Winterhager E, Van Roy F, Mareel MM et al. Loss of epithelial differentiation and gain of invasiveness correlates with tyrosine phosphorylation of the E-cadherin/beta-catenin complex in cells transformed with a temperature-sensitive v-SRC gene. J Cell Biol 1993; 120: 757–766. [PubMed: 8425900]
13. Nelson WJ, Nusse R. Convergence of Wnt, beta-catenin, and cadherin pathways. Science 2004; 303: 1483–1487. [PubMed: 15001769]
14. Enslen H, Raingeaud J, Davis RJ. Selective activation of p38 mitogen-activated protein (MAP) kinase isoforms by the MAP kinase kinases MKK3 and MKK6. J Biol Chem 1998; 273: 1741–1748. [PubMed: 9430721]
15. Cuadrado A, Nebreda AR. Mechanisms and functions of p38 MAPK signalling. Biochem J 2010; 429: 403–417. [PubMed: 20626350]
16. Shi Y, Gaestel M. In the cellular garden of forking paths: how p38 MAPKs signal for downstream assistance. Biol Chem 2002; 383: 1519–1536. [PubMed: 12452429]
17. Gantke T, Sriskantharajah S, Sadowski M, Ley SC. IkappaB kinase regulation of the TPL-2/ERK MAPK pathway. Immunol Rev 2012; 246: 168–182. [PubMed: 22435554]
18. Salmeron A, Ahmad TB, Carlile GW, Pappin D, Narsimhan RP, Ley SC. Activation of MEK-1 and SEK-1 by Tpl-2 proto-oncoprotein, a novel MAP kinase kinase kinase. EMBO J 1996; 15: 817–826. [PubMed: 8631303]
19. Dumitru CD, Ceci JD, Tsatsanis C, Kontoyiannis D, Stamatakis K, Lin JH et al. TNF-alpha induction by LPS is regulated posttranscriptionally via a Tpl2/ERK-dependent pathway. Cell 2000; 103: 1071–1083. [PubMed: 11163183]
20. Pattison MJ, Mitchell O, Flynn HR, Chen CS, Yang HT, Ben-Addi H et al. TLR and TNF-R1 activation of the MKK3/MKK6-p38alpha axis in macrophages is mediated by TPL-2 kinase. Biochem J 2016; 473: 2845–2861. [PubMed: 27402796]
21. Senger K, Pham VC, Varfolomeev E, Hackney JA, Corzo CA, Collier J et al. The kinase TPL2 activates ERK and p38 signaling to promote neutrophilic inflammation. Sci Signal 2017; 10.
22. Gong J, Fang C, Zhang P, Wang PX, Qiu Y, Shen LJ et al. Tumor Progression Locus 2 in Hepatocytes Potentiates Both Liver and Systemic Metabolic Disorders in Mice. Hepatology 2019; 69: 524–544. [PubMed: 29381809]
23. Beinke S, Robinson MJ, Hugunin M, Ley SC. Lipopolysaccharide activation of the TPL-2/MEK/extracellular signal-regulated kinase mitogen-activated protein kinase cascade is regulated by IkappaB kinase-induced proteolysis of NF-kappaB1 p105. Mol Cell Biol 2004; 24: 9658–9667. [PubMed: 15485931]
24. Dodhiawala PB, Khurana N, Zhang D, Cheng Y, Li L, Wei Q et al. TPL2 enforces RAS-induced inflammatory signaling and is activated by point mutations. J Clin Invest 2020.
25. Cho J, Melnick M, Solidakis GP, Tsichlis PN. Tpl2 (tumor progression locus 2) phosphorylation at Thr290 is induced by lipopolysaccharide via an Ikappa-B Kinase-beta-dependent pathway and is required for Tpl2 activation by external signals. J Biol Chem 2005; 280: 20442–20448. [PubMed: 15778223]
26. Bulavin DV, Fornace AJ Jr. p38 MAP kinase's emerging role as a tumor suppressor. Adv Cancer Res 2004; 92: 95–118. [PubMed: 15530558]

27. Zheng H, Seit-Nebi A, Han X, Aslanian A, Tat J, Liao R et al. A posttranslational modification cascade involving p38, Tip60, and PRAK mediates oncogene-induced senescence. Mol Cell 2013; 50: 699–710. [PubMed: 23685072]
28. Ellinger-Ziegelbauer H, Kelly K, Siebenlist U. Cell cycle arrest and reversion of Ras-induced transformation by a conditionally activated form of mitogen-activated protein kinase kinase kinase 3. Mol Cell Biol 1999; 19: 3857–3868. [PubMed: 10207109]
29. She QB, Bode AM, Ma WY, Chen NY, Dong Z. Resveratrol-induced activation of p53 and apoptosis is mediated by extracellular-signal-regulated protein kinases and p38 kinase. Cancer Res 2001; 61: 1604–1610. [PubMed: 11245472]
30. Wen HC, Avivar-Valderas A, Sosa MS, Girnius N, Farias EF, Davis RJ et al. p38alpha Signaling Induces Anoikis and Lumen Formation During Mammary Morphogenesis. Sci Signal 2011; 4: ra34. [PubMed: 21610252]
31. Huang S, New L, Pan Z, Han J, Nemerow GR. Urokinase plasminogen activator/urokinase-specific surface receptor expression and matrix invasion by breast cancer cells requires constitutive p38alpha mitogen-activated protein kinase activity. J Biol Chem 2000; 275: 12266–12272. [PubMed: 10766865]
32. Anwar T, Arellano-Garcia C, Ropa J, Chen YC, Kim HS, Yoon E et al. p38-mediated phosphorylation at T367 induces EZH2 cytoplasmic localization to promote breast cancer metastasis. Nat Commun 2018; 9: 2801. [PubMed: 30022044]
33. Wu MZ, Chen SF, Nieh S, Benner C, Ger LP, Jan CI et al. Hypoxia Drives Breast Tumor Malignancy through a TET-TNFalpha-p38-MAPK Signaling Axis. Cancer Res 2015; 75: 3912–3924. [PubMed: 26294212]
34. Harper KL, Sosa MS, Entenberg D, Hosseini H, Cheung JF, Nobre R et al. Mechanism of early dissemination and metastasis in Her2(+) mammary cancer. Nature 2016; 540: 588–592. [PubMed: 27974798]
35. Kim G, Khanal P, Kim JY, Yun HJ, Lim SC, Shim JH et al. COT phosphorylates prolyl-isomerase Pin1 to promote tumorigenesis in breast cancer. Mol Carcinog 2015; 54: 440–448. [PubMed: 24265246]
36. Kim K, Kim G, Kim JY, Yun HJ, Lim SC, Choi HS. Interleukin-22 promotes epithelial cell transformation and breast tumorigenesis via MAP3K8 activation. Carcinogenesis 2014; 35: 1352–1361. [PubMed: 24517997]
37. Decicco-Skinner KL, Trovato EL, Simmons JK, Lepage PK, Wiest JS. Loss of tumor progression locus 2 (tpl2) enhances tumorigenesis and inflammation in two-stage skin carcinogenesis. Oncogene 2011; 30: 389–397. [PubMed: 20935675]
38. Gkirtzimanaki K, Gkouskou KK, Oleksiewicz U, Nikolaidis G, Vyrla D, Liontos M et al. TPL2 kinase is a suppressor of lung carcinogenesis. Proc Natl Acad Sci U S A 2013; 110: E1470–1479. [PubMed: 23533274]
39. Muthuswamy SK, Li D, Lelievre S, Bissell MJ, Brugge JS. ErbB2, but not ErbB1, reinitiates proliferation and induces luminal repopulation in epithelial acini. Nat Cell Biol 2001; 3: 785–792. [PubMed: 11533657]
40. Husemann Y, Geigl JB, Schubert F, Musiani P, Meyer M, Burghart E et al. Systemic spread is an early step in breast cancer. Cancer Cell 2008; 13: 58–68. [PubMed: 18167340]
41. Mani SA, Guo W, Liao MJ, Eaton EN, Ayyanan A, Zhou AY et al. The epithelial-mesenchymal transition generates cells with properties of stem cells. Cell 2008; 133: 704–715. [PubMed: 18485877]
42. Xu L, Chen S, Bergan RC. MAPKAPK2 and HSP27 are downstream effectors of p38 MAP kinase-mediated matrix metalloproteinase type 2 activation and cell invasion in human prostate cancer. Oncogene 2006; 25: 2987–2998. [PubMed: 16407830]
43. Han Y, Zhang L, Wang W, Li J, Song M. Livin promotes the progression and metastasis of breast cancer through the regulation of epithelialmesenchymal transition via the p38/GSK3beta pathway. Oncol Rep 2017; 38: 3574–3582. [PubMed: 29039608]
44. Yan MH, Hao JH, Zhang XG, Shen CC, Zhang DJ, Zhang KS et al. Advancement in TPL2-regulated innate immune response. Immunobiology 2019; 224: 383–387. [PubMed: 30853309]

45. Slack DN, Seternes OM, Gabrielsen M, Keyse SM. Distinct binding determinants for ERK2/p38alpha and JNK map kinases mediate catalytic activation and substrate selectivity of map kinase phosphatase-1. J Biol Chem 2001; 276: 16491–16500. [PubMed: 11278799]
46. Candas D, Lu CL, Fan M, Chuang FY, Sweeney C, Borowsky AD et al. Mitochondrial MKP1 is a target for therapy-resistant HER2-positive breast cancer cells. Cancer Res 2014; 74: 7498–7509. [PubMed: 25377473]
47. Mamillapalli R, Gavrilova N, Mihaylova VT, Tsvetkov LM, Wu H, Zhang H et al. PTEN regulates the ubiquitin-dependent degradation of the CDK inhibitor p27(KIP1) through the ubiquitin E3 ligase SCF(SKP2). Curr Biol 2001; 11: 263–267. [PubMed: 11250155]
48. Gao D, Inuzuka H, Tseng A, Chin RY, Toker A, Wei W. Phosphorylation by Akt1 promotes cytoplasmic localization of Skp2 and impairs APCCdh1-mediated Skp2 destruction. Nat Cell Biol 2009; 11: 397–408. [PubMed: 19270695]
49. Lin HK, Wang G, Chen Z, Teruya-Feldstein J, Liu Y, Chan CH et al. Phosphorylation-dependent regulation of cytosolic localization and oncogenic function of Skp2 by Akt/PKB. Nat Cell Biol 2009; 11: 420–432. [PubMed: 19270694]
50. Chan CH, Li CF, Yang WL, Gao Y, Lee SW, Feng Z et al. The Skp2-SCF E3 ligase regulates Akt ubiquitination, glycolysis, herceptin sensitivity, and tumorigenesis. Cell 2012; 149: 1098–1111. [PubMed: 22632973]
51. Ruiz-Saenz A, Dreyer C, Campbell MR, Steri V, Gulizia N, Moasser MM. HER2 Amplification in Tumors Activates PI3K/Akt Signaling Independent of HER3. Cancer Res 2018; 78: 3645–3658. [PubMed: 29760043]
52. Wisinski KB, Tevaarwerk AJ, Burkard ME, Rampurwala M, Eickhoff J, Bell MC et al. Phase I Study of an AKT Inhibitor (MK-2206) Combined with Lapatinib in Adult Solid Tumors Followed by Dose Expansion in Advanced HER2+ Breast Cancer. Clin Cancer Res 2016; 22: 2659–2667. [PubMed: 27026198]
53. Krcova Z, Ehrmann J, Krejci V, Eliopoulos A, Kolar Z. Tpl-2/Cot and COX-2 in breast cancer. Biomed Pap Med Fac Univ Palacky Olomouc Czech Repub 2008; 152: 21–25. [PubMed: 18795070]
54. del Barco Barrantes I, Nebreda AR. Roles of p38 MAPKs in invasion and metastasis. Biochem Soc Trans 2012; 40: 79–84. [PubMed: 22260669]
55. Sosa MS, Avivar-Valderas A, Bragado P, Wen HC, Aguirre-Ghiso JA. ERK1/2 and p38alpha/beta signaling in tumor cell quiescence: opportunities to control dormant residual disease. Clin Cancer Res 2011; 17: 5850–5857. [PubMed: 21673068]
56. Chan CH, Lee SW, Wang J, Lin HK. Regulation of Skp2 expression and activity and its role in cancer progression. ScientificWorldJournal 2010; 10: 1001–1015. [PubMed: 20526532]
57. Weidensdorfer D, Stohr N, Baude A, Lederer M, Kohn M, Schierhorn A et al. Control of c-myc mRNA stability by IGF2BP1-associated cytoplasmic RNPs. RNA 2009; 15: 104–115. [PubMed: 19029303]
58. Kato H, Asamitsu K, Sun W, Kitajima S, Yoshizawa-Sugata N, Okamoto T et al. Cancer-derived UTX TPR mutations G137V and D336G impair interaction with MLL3/4 complexes and affect UTX subcellular localization. Oncogene 2020; 39: 3322–3335. [PubMed: 32071397]
59. Wei W, Shin YS, Xue M, Matsutani T, Masui K, Yang H et al. Single-Cell Phosphoproteomics Resolves Adaptive Signaling Dynamics and Informs Targeted Combination Therapy in Glioblastoma. Cancer Cell 2016; 29: 563–573. [PubMed: 27070703]

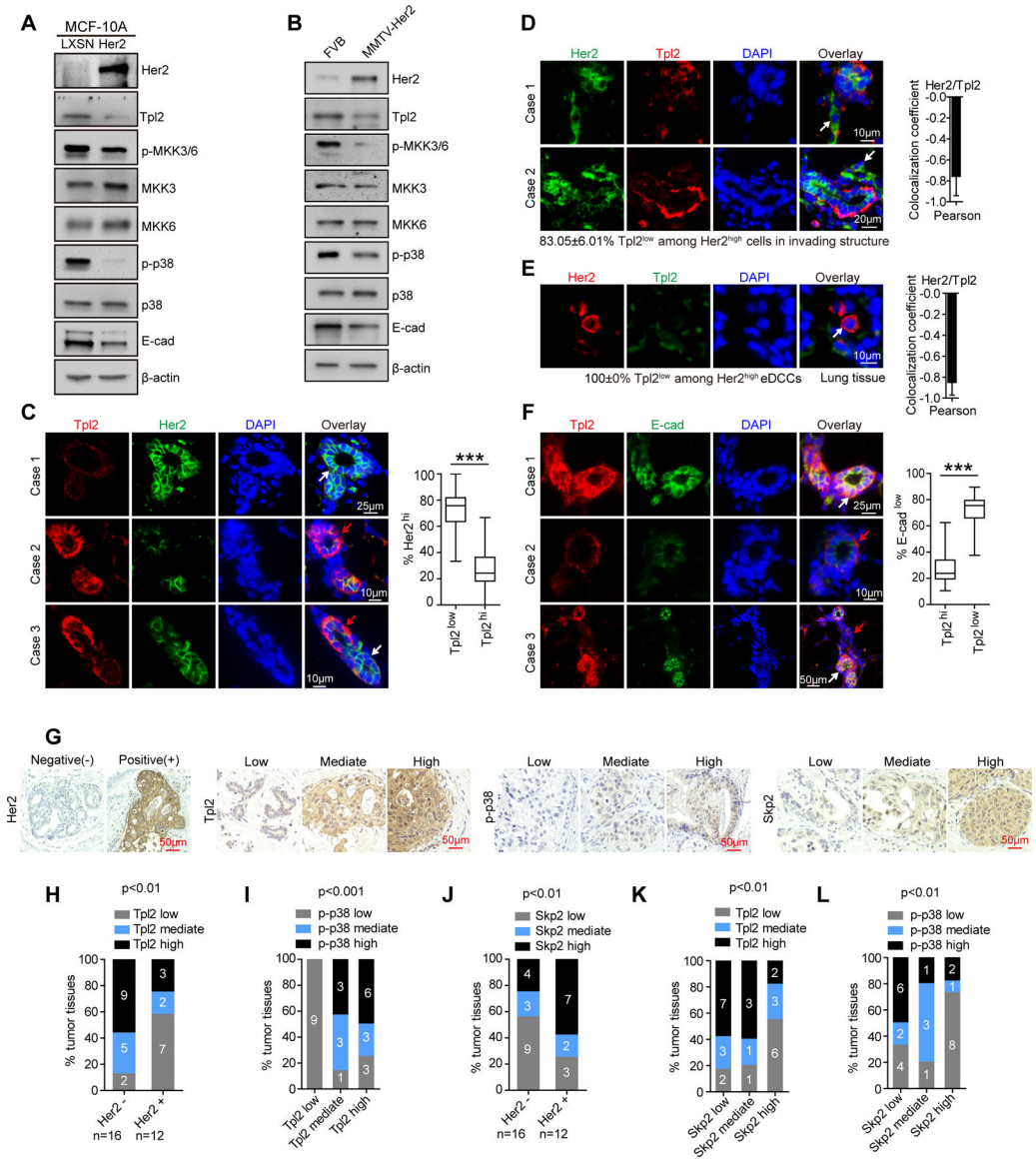

Fig. 1.

Reduced Tpl2 levels correlate with Her2^{+} status and reduced p38 activation in cell and mouse models of early lesion breast cancer and early-lesion human breast cancer tissues, and with increased Skp2 expression in early-lesion human breast cancer tissues.

(A–B) Western blot analysis of MCF-10A and MCF-10A-Her2 cells (A) and mammary epithelial cells isolated from 14–18-week-old wild type FVB mice (FVB) or MMTV-Her2 mice with breast cancer early lesions (MMTV-Her2) (B).

(C) Mammary glands from 14–18-week-old MMTV-Her2 mice with early lesion breast cancer was co-staining for Her2 and Tpl2 by immunofluorescence. Photos of representative ducts containing mainly Her2^{high}Tpl2^{low} (case1) or Her2^{low}Tpl2^{high} (case2) cells or both (case3) were shown (left). White arrows, Her2^{high}Tpl2^{low} cells, red arrows, Her2^{low}Tpl2^{high} cells. Percentage of Her2^{high} cells that were Tpl2^{low} or Tpl2^{high} were quantified (mean±SD, n=2 × 32 ducts from 2 mice, at least 5–30 Her2^{high} cells/duct counted) (right).

(D) Representative images of 14–18-week-old MMTV-Her2 mouse mammary ducts co-stained for Her2 and Tpl2 by immunofluorescence, showing $Her2^{high}Tpl2^{low}$ cells in invading buds (white arrows) and percentage of $Her2^{high}$ cells in invading buds that are $Tpl2^{low}$ (mean±SD, n=2 mice, 40 cells/section counted).
(E) Representative images of eDCCs in the lungs of 14–18-week-old MMTV-Her2 mice co-stained for Her2 and Tpl2, showing $Her2^{high}Tpl2^{low}$ eDCCs (white arrows) and percentage of $Her2^{high}$ eDCCs that are $Tpl2^{low}$ (mean±SD, n=2 mice, 13 cells/section counted).
(D–E) Bar graphs (right) show Pearson's correlation coefficient (PCC) for $Her2^{high}$ and $Tpl2^{low}$ analyzed in 20 (D) or 13 (E) $Her2^{high}$ cells/mouse (2 mice) using ImageJ.
(F) Representative images of 14–18-week-old MMTV-Her2 mouse mammary ducts containing mainly $Tpl2^{high}$E-cad^{high} (case1) or $Tpl2^{low}$E-cad^{low} (case2) cells or both (case3) (left). White arrows, $Tpl2^{high}$E-cad^{high} cells; red arrows, $Tpl2^{low}$E-cad^{low} cells. Percentage of E-cad^{low} cells that were $Tpl2^{low}$ or $Tpl2^{high}$ were quantified (mean±SD, n=2 × 30 ducts from 2 mice, at least 3–30 E-cad^{low} cells/duct counted) (right).
(G) Representative images of early-lesion human breast cancer tissues with $Her2^{+}$ or $Her2^{-}$ status and low, mediate and high IP scores for Tpl2, p-p38 and Skp2 determined by IHC.
(H, J) Quantification of percentage of $Her2^{-}$ and $Her2^{+}$ early-lesion human breast cancer tissues with low, mediate or high IHC scores of Tpl2 (H) or Skp2 (J).
(I, K–L) Quantification of percentage of early-lesion human breast cancer tissues with low, mediate or high IHC scores of p-p38 (I), Tpl2 (K) or p-p38 (L) in groups of samples with low, mediate or high scores of Tpl2 (I) or Skp2 (K, L), respectively.
(C, F) ***$p<0.001$ vs indicated controls in one-sided Mann-Whitney *U*-test.
(H–L) Numbers in bars indicate number of cases in each category. p values were from Chi-square χ^2 test.

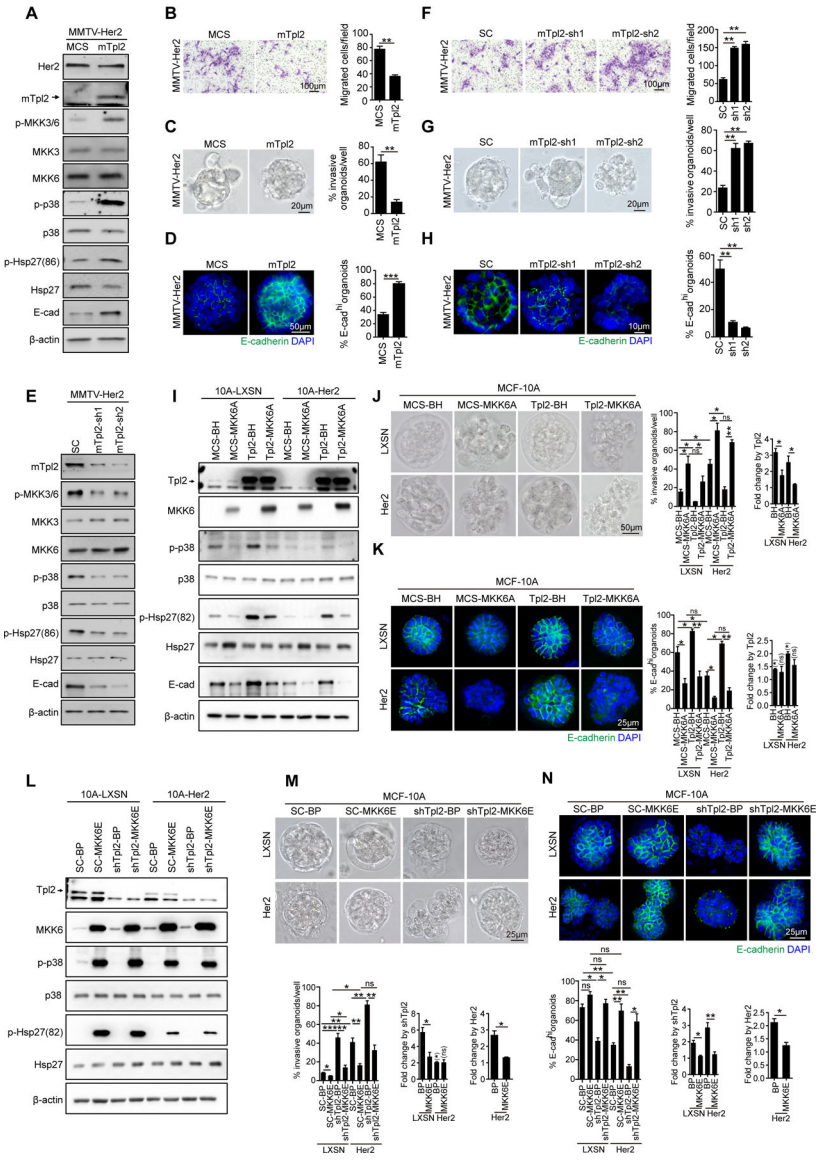

Fig. 2.

Her2 mediates migration, invasion and EMT by downregulating Tpl2 expression in mammary epithelial cells isolated from 14–18-week-old MMTV-Her2 mice with early lesions.

(A–D) MMTV-Her2 cells were transduced with vector (MCS) or Tpl2 and analyzed for protein expressions (A), migration (B), percentage of 8-day organoids with outward invading cells (C), and percentage of 8-day organoids with high-intensity E-cadherin junctions (D).

(E–H) MMTV-Her2 cells were transduced with a scrambled shRNA (SC) or Tpl2 shRNAs (Tpl2-sh1 and -sh2) and analyzed for protein expressions (E), migration (F), percentage of 8-day organoids with outward invading cells (G), and percentage of 8-day organoids with high-intensity E-cadherin junctions by immunofluorescence staining (H).

(I–K) MCF-10A cells transduced with Her2 or vector (LXSN), Tpl2 or vector (MCS) and MKK6A or vector (BH) were analyzed for protein expressions (I), percentage of 8-day

organoids with outward invading cells (J), and percentage of 8-day organoids with high-intensity E-cadherin junctions (K).

(L–N) MCF-10A cells transduced with Her2 or vector (LXSN), Tpl2 shRNA or scrambled shRNA (SC) and MKK6E or vector (BP) were analyzed for protein expressions (L), percentage of 8-day organoids with outward invading cells (M), and percentage of 8-day organoids with high-intensity E-cadherin junctions (N).

(B–D, F–H, J–K, M–N) Representative images (left) and indicated quantifications of results (right) are shown. Numbers are mean±SD for duplicates (D, H, K, N) or triplicates (B-C, F-G, J, M). Fold changes (mean±SD) by Her2 (L-N), Tpl2 (I-K) or shTpl2 (L-N) were calculated and compared between indicated groups. ns, not significant, *p<0.05, **p<0.01, ***p<0.001 vs indicated controls in one-sided unpaired *t*-test. p values in parentheses represent those for the fold change itself.

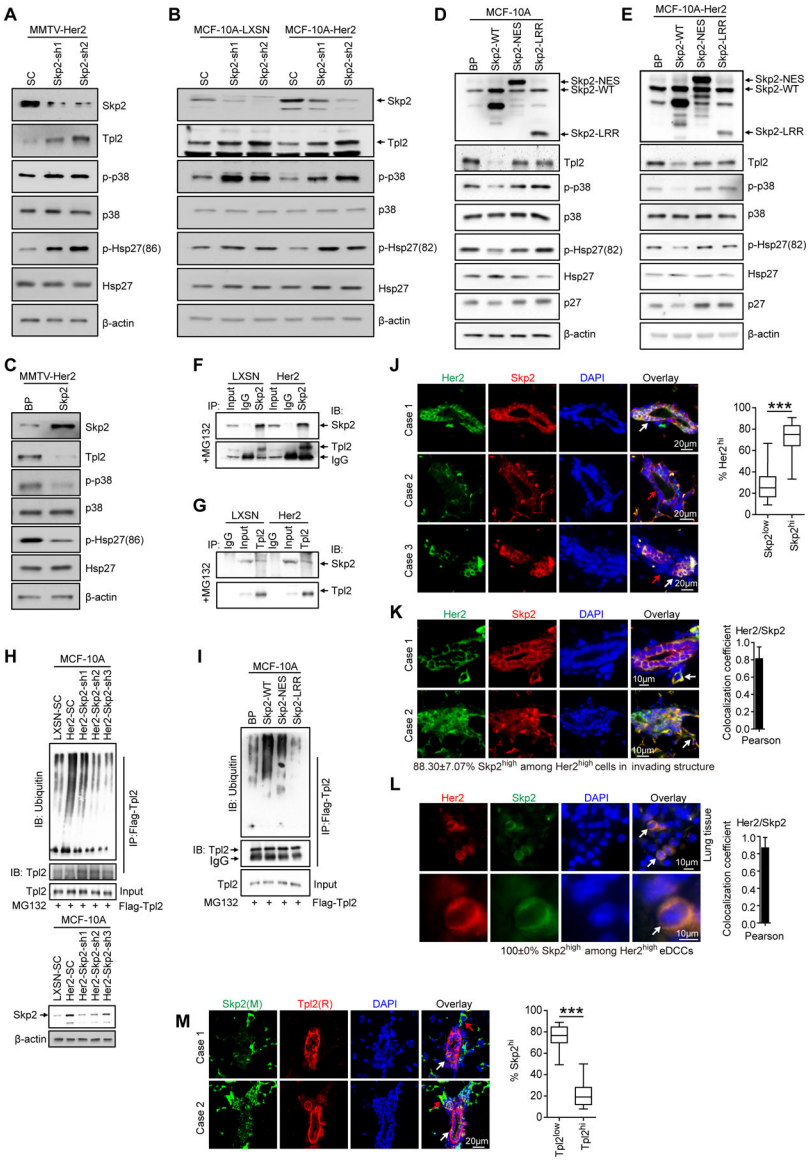

Fig. 3.

Her2 reduces Tpl2 protein expression through Skp2-mediated ubiquitination and proteasomal degradation.

(A–B) Western blot analysis of mammary epithelial cells from 14–18-week-old MMTV-Her2 mice (A) and MCF-10A or MCF-10A-Her2 cells (B) transduced with a scrambled shRNA (SC) or Skp2 shRNA. Fold Changes (mean±SD) by Her2 in Tpl2, p-p38 and p-Hsp27 were calculated and compared between indicated groups (B). *p<0.05, **p<0.01 vs indicated controls in one-sided unpaired *t*-test.

(C) Western blot analysis of mammary epithelial cells from 14–18-week-old MMTV-Her2 mice transduced with wild type Skp2 (Skp2-WT).

(D–E) Western blot analysis of MCF-10A (D) or MCF-10A-Her2 (E) cells transduced with vector (BP), wild type Skp2 (Skp2-WT) or catalytically inactive Skp2 mutants (Skp2-NES and -LRR).

(F–G) Co-immunoprecipitation analysis of Skp2-Tpl2 interaction. Skp2 (F) or Tpl2 (G) was immunoprecipitated from MG132-treated MCF-10A-LXSN or MCF-10A-Her2 cells by respective antibody or IgG as control. Immunoprecipitates were analyzed by Western blotting along with inputs.

(H–I) Flag-Tpl2 was immunoprecipitated by an anti-Flag antibody after 8h of MG132 treatment from MCF-10A-LXSN or MCF-10A-Her2 cells transduced with Flag-Tpl2 and a scrambled shRNA (SC) or Skp2 shRNA (sh1–3) (H) or from MCF-10A cells transduced with Flag-Tpl2 and wild type (WT) or E3 ligase-dead mutants (-NES and -LRR) of Skp2 (I) and analyzed by Western blotting to detect ubiquitylated Tpl2 using an anti-ubiquitin antibody.

(J) Representative image of mammary glands from 14–18-week-old MMTV-Her2 mice co-stained for Her2 and Skp2 by immunofluorescence, showing representative ducts containing mainly $Her2^{high}Skp2^{high}$ (case1) or $Her2^{low}Skp2^{low}$ (case2) cells or both (case3) were shown (left). White arrows, $Her2^{high}Skp2^{high}$ cells, red arrows, $Her2^{low}Skp2^{low}$ cells. Percentage of $Her2^{high}$ cells that were $Skp2^{low}$ or $Skp2^{high}$ were quantified (mean±SD, n=2 × 34 ducts from 2 mice, at least 5–30 $Her2^{high}$ cells/duct counted) (right).

(K) Representative images of 14–18-week-old MMTV-Her2 mouse mammary ducts co-stained for Her2 and Skp2 by immunofluorescence, showing $Her2^{high}Skp2^{high}$ cells in the early lesions (white arrows) and percentage of $Her2^{high}$ cells in invading buds that were $Skp2^{high}$ (mean±SD, n=2 mice, 50 cells/section counted) (bottom).

(L) Representative images of eDCCs in the lungs of 14–18-week-old MMTV-Her2 mice co-stained for Her2 and Skp2, showing $Her2^{high}Skp2^{high}$ eDCCs (white arrows) and percentage of $Her2^{high}$ eDCCs that were $Skp2^{high}$.

(K–L) Bar graphs (right) show Pearson's correlation coefficient (PCC) for $Her2^{high}$ and $Skp2^{high}$ analyzed in 20 (K) or 12 (L) $Her2^{high}$ cells/mouse (2 mice) using ImageJ.

(M) Representative image of mammary glands from 14–18-week-old MMTV-Her2 mice co-stained for Skp2 and Tpl2, showing 2 representative ducts containing $Skp2^{high}Tpl2^{low}$ (red arrows) and $Skp2^{low}Tpl2^{high}$ (white arrows) cells. Percentage of $Skp2^{high}$ cells that were $Tpl2^{low}$ or $Tpl2^{high}$ were quantified (mean±SD, n=2 × 20 ducts from 2 mice, at least 5–30 $Skp2^{high}$ cells/duct counted) (right).

(J, M) ***$p<0.001$ vs indicated controls in one-sided Mann-Whitney *U*-test.

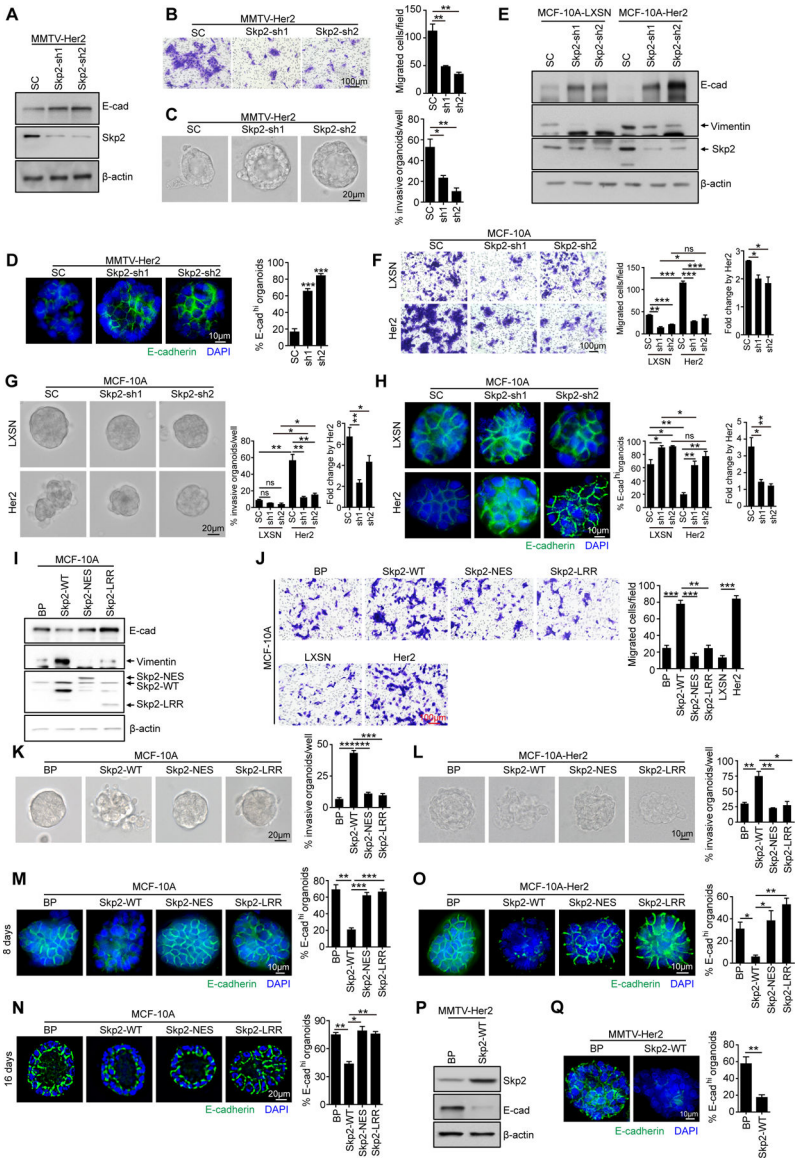

Fig. 4.

Skp2 mediates Her2-induced Tpl2 and p38 suppression and migration, invasion and EMT in early lesion breast cancer cells.

(A–H) Mammary epithelial cells from 14–18-week-old MMTV-Her2 mice (A–D) or MCF-10A and MCF-10A-Her2 cells (E–H) transduced with a scrambled shRNA (SC) or Skp2 shRNAs were analyzed for protein expressions (A, E), migration (B, F), percentage of 8-day invasive organoids (C, G), and percentage of 8-day organoids with high-intensity E-cadherin junctions (D, H).

(I–O) MCF-10A and/or MCF-10A-Her2 cells transduced with vector (BP) or wild type (WT) or enzyme-dead mutants (Skp2-NES and -LRR) of Skp2 were analyzed for protein expression (I), migration (J), percentage of 8-day invasive organoids (K–L), and percentage of 8-day (M, O) and 16-day (N) organoids with high-intensity E-cadherin junctions.

(P–Q) Mammary epithelial cells isolated from 14–18-week-old MMTV-Her2 mice transduced with vector (BP) or wild type Skp2 (Skp2-WT) were analyzed for protein expression (P) and percentage of 8-day organoids with high-intensity E-cadherin junctions (Q).

(B–D, F-H, J-O, Q) Representative images (left) and indicated quantifications of results (right) are shown. Numbers are mean±SD for duplicates (D, H, M-O, Q) or triplicates (B–C, F-G, J-L). Fold Change (mean±SD) by Her2 was calculated and compared between indicated groups. ns, not significant, *P<0.05, **P<0.01 and ***P<0.001 vs indicated controls in one-sided, unpaired *t*-test.

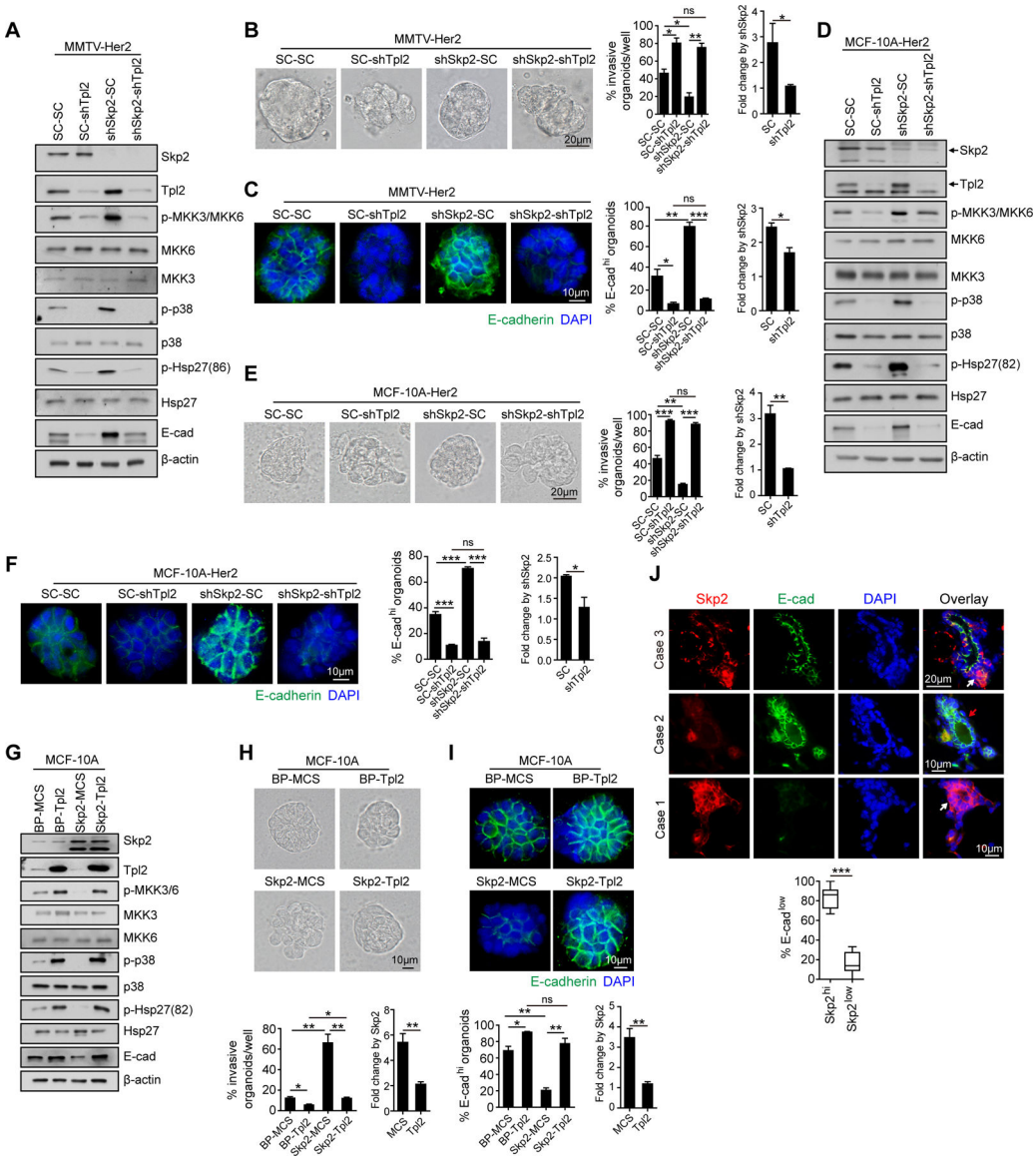

Fig. 5.

Skp2 promotes migration, invasion and EMT by suppressing Tpl2 in Her2^{+} early lesion breast cancer cells.

(A–F) Mammary epithelial cells isolated from 14–18-week-old MMTV-Her2 mice (A–C) or MCF-10A-Her2 cells (D–F) were transduced with a scrambled shRNA (SC) or Skp2 shRNA (shSkp2) (with puromycin-resistance) and a scrambled shRNA (SC) or Tpl2 shRNA (shTpl2) (with blasticidin-resistance) and analyzed for the status of the p38 pathway and E-cadherin (A, D), percentage of 8-day invasive organoids (B, E), and percentage of 8-day organoids with high-intensity E-cadherin junctions (C, F).

(G–I) MCF-10A cells transduced with vector (BP) or wild type Skp2 and vector (MCS) or Tpl2 were analyzed for the status of the p38 pathway (G), percentage of 8-day invasive organoids (H), and percentage of 8-day organoids with high-intensity E-cadherin junctions (I).

(B–C, E-F, H-I) Representative images (left) and indicated quantifications of results (right) are shown. Numbers are mean±SD for triplicates (B, E, H) or duplicates (C, F, I). Fold Change (mean±SD) by shSkp2 (A–F) or Skp2 (G–I) were calculated and compared between indicated groups. ns, not significant, *P<0.05, **P<0.01, ***P<0.001 vs indicated controls in one-sided unpaired *t*-test.

(J) Representative image of mammary glands from 14–18-week-old MMTV-Her2 mice co-stained for Skp2 and E-cadherin by immunofluorescence, showing representative ducts containing mainly $Skp2^{high}E\text{-}cad^{low}$ (case1) or $Skp2^{low}E\text{-}cad^{high}$ (case2) cells or both (case3). White arrows, $Skp2^{high}E\text{-}cad^{low}$ cells, red arrows, $Skp2^{low}E\text{-}cad^{high}$ cells. Percentage of $E\text{-}cadherin^{low}$ cells that were $Skp2^{high}$ or $Skp2^{low}$ were quantified (mean±SD, n=2 × 20 ducts from 2 mice, at least 3–30 $E\text{-}cad^{low}$ cells/duct counted) (right). *** P<0.001 vs indicated controls in one-sided Mann-Whitney *U*-test.

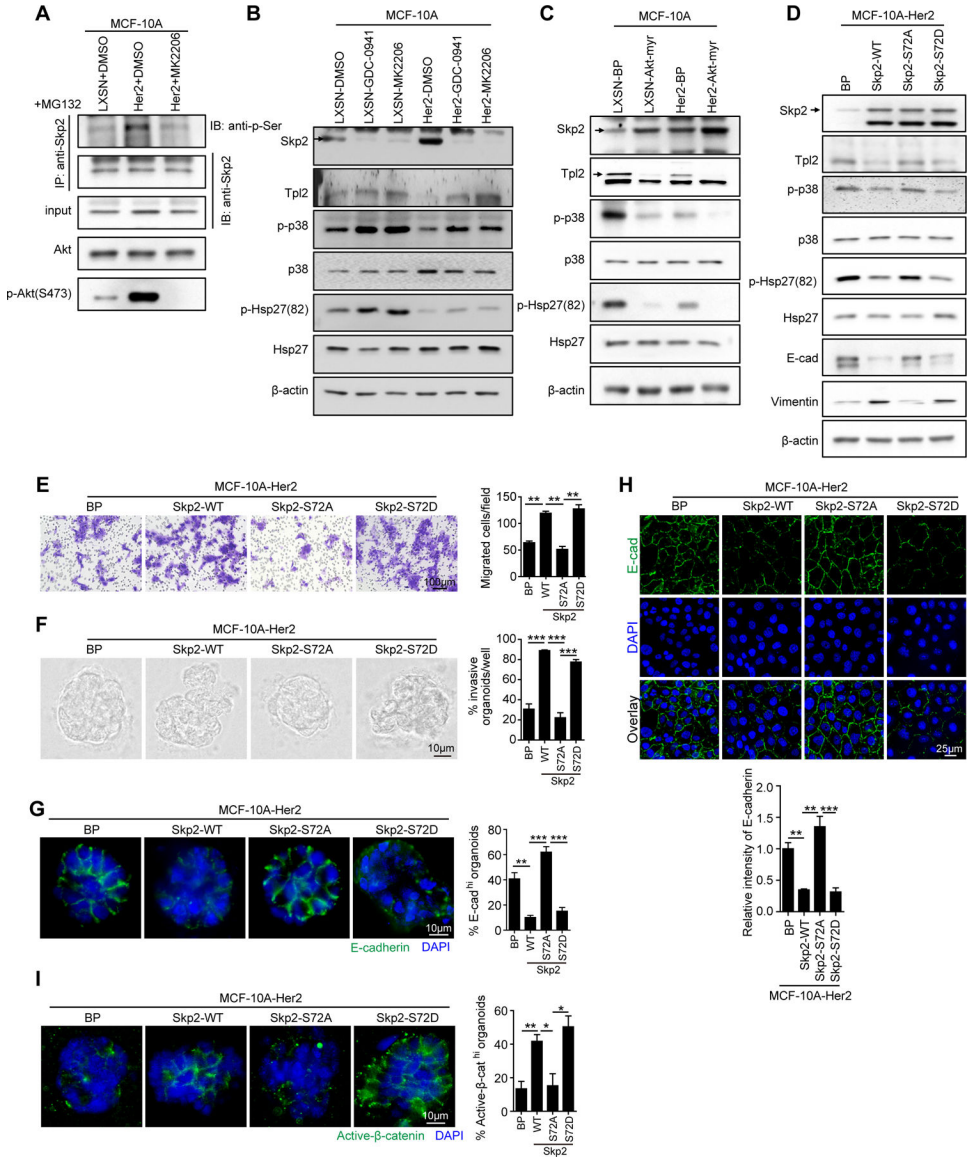

Fig. 6.

Her2 induces Skp2 expression and function through Akt-mediated phosphorylation.

(A) Her2-induced serine-phosphorylation of Skp2 requires Akt. Western blot analysis of Skp2 immunoprecipitated from MG132-treated MCF-10A or MCF-10A-Her2 cells treated with an Akt inhibitor MK2206.

(B–D) Western blot analysis of MCF-10A or MCF-10A-Her2 cells treated with a PI3K inhibitor GDC0941 (1 μM) or Akt inhibitor MK2206 (5 μM) for 24 hours (B), MCF-10A or MCF-10A-Her2 cells transduced with vector (BP) or myristoylated constitutively active Akt (Akt-myr) (C), or MCF-10A-Her2 cells transduced with wild type (Skp2-WT) or nonphosphorylatable (Skp2-S72A) or phosphomimetic (Skp2-S72D) mutant of Skp2 (D), detecting the level of Skp2 and status of the p38 pathway. Fold Change (mean±SD) by Her2 was calculated and compared between indicated groups (B). ns, not significant, *p<0.05 vs indicated controls in one-sided unpaired *t*-test.

(E–I) MCF-10A-Her2 cells transduced with wild type Skp2 (Skp2-WT) or the S72A or S72D mutant of Skp2 were analyzed for migration (E), percentage of 8-day invasive organoids (F), and E-cadherin junctions in 8-day organoids (G) and 2D cultures (H) and active β-catenin levels (I) by immunofluorescence staining.

(E–G, I) Representative images (left) and indicated quantifications of results (right) are shown. Numbers are mean±SD for triplicates (E–F) or duplicates (G, I).

(H) Representative images (top) and quantifications of results (bottom) are shown. Values are mean±SD of E-cadherin fluorescence intensity from 6 random fields from each of the triplicates after normalization to that of MCF-10A-Her2-BP.

(E–I) *P<0.05, **P<0.01, ***P<0.001 vs indicated controls in one-sided unpaired *t*-test.

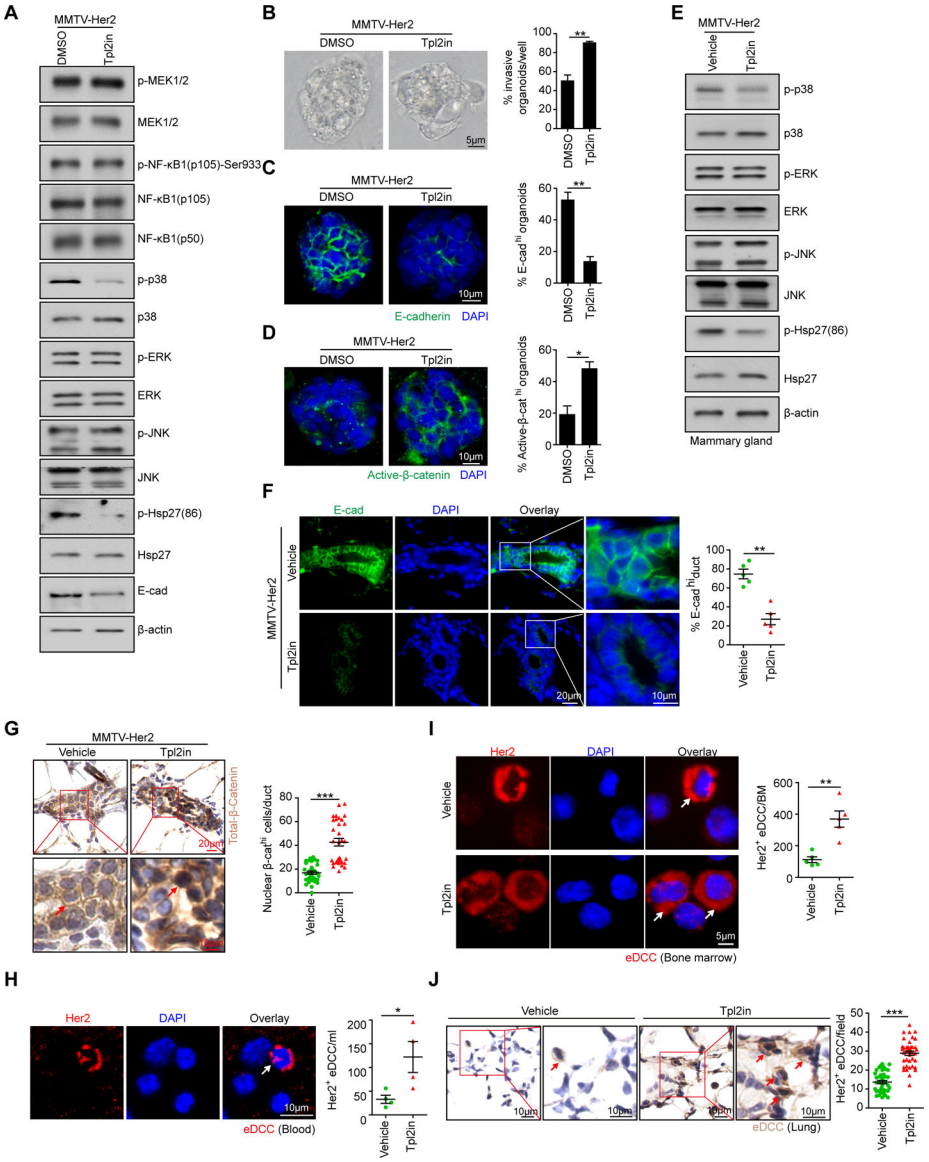

Fig. 7.

Pharmacological inhibition of Tpl2 suppresses the p38 pathway and promotes the disseminating phenotypes in Her2^{+} early lesion breast cancer cells and enhances early dissemination in vivo in the MMTV-Her2 mouse model.

(A) Mammospheres isolated from 14–18-week-old MMTV-Her2 mice with early lesions were treated with the Tpl2 inhibitor (1 μM) for 24 h and analyzed by Western blotting.

(B–D) Mammospheres isolated from 14–18-week-old MMTV-Her2 mice were seeded in 3D Matrigel, treated with the Tpl2 inhibitor (1 μM) 6 days after seeding for 6 days with medium replenishment every day, and analyzed for percentage of invasive organoids (B), E-cadherin junctions (C) and active β-catenin levels (D). Representative images (left) and indicated quantifications of results (right) are shown. Numbers are mean±SD for triplicates (B) or duplicates (C, D).

(E) Western blot analysis of mammospheres isolated from MMTV-Her2 mice treated with vehicle or the Tpl2 inhibitor (Tpl2in) for two weeks starting from 14–18 weeks of age.
(F–G) Sections of mammary glands from MMTV-Her2 mice treated with vehicle or the Tpl2 inhibitor (Tpl2in) for two weeks starting from 14–18 weeks of age were stained for E-cadherin (F) or total β-catenin (G) by IF and IHC, respectively. Images of representative ducts and magnified areas are shown on the left. Percentage of E-cad^{high} ducts (mean±SD, n=90 ducts from 4 mice/group) (F) and percentage of nuclear β-cat^{high} cells/duct (mean±SD, n=40 ducts from 3 mice/group, 20–100 cells per duct were counted) (G) were quantified (right).
(H–I) Early disseminating cancer cells (eDCCs) purified from blood (H) and bone marrow (I) of 14–18-week-old MMTV-Her2 mice treated with vehicle or the Tpl2 inhibitor (Tpl2in) for two weeks were stained for Her2 by immunofluorescence in cytospin preparations. Representative images are shown with arrows indicating Her2^{+} eDCCs (left). Number of Her2^{+} eDCCs per ml of blood (H) or per bone marrow (I) were quantified (right). Lines are mean±SD, n=4 mice (H) or 5 mice (I).
(J) Lung sections from 14–18-week-old MMTV-Her2 mice treated with vehicle or the Tpl2 inhibitor (Tpl2in) for two weeks were stained for Her2 by IHC. Representative images and magnified areas are shown with arrows indicating Her2^{+} eDCCs (left). Number of Her2^{+} eDCCs/field were quantified (right). Lines are mean±SD, n=40 fields from 4 mice/group. *P<0.05, **P<0.01, ***P<0.001 vs indicated controls in one sided unpaired *t*-test (B–D) or one-sided Mann-Whitney *U*-test (F–J).